

An experimental assessment of the evaporation correlations for natural, forced and combined convection regimes

A Jodat* and M Moghiman

Faculty of Engineering, Ferdowsi University of Mashhad, Mashhad, Iran

The manuscript was received on 9 September 2010 and was accepted after revision for publication on 26 May 2011.

DOI: 10.1177/0954406211413961

Abstract: In the present study, the applicability of widely used evaporation models (Dalton approach-based correlations) is experimentally investigated for natural, forced, and combined convection regimes. A series of experimental measurements are carried out over a wide range of water temperatures and air velocities for $0.01 \leq Gr/Re^2 \leq 100$ in a heated rectangular pool. The investigations show that the evaporation rate strongly depends on the convection regime's Gr/Re^2 value. The results show that the evaporation rate increases with the difference in vapour pressures over both forced convection ($0.01 \leq Gr/Re^2 \leq 0.1$) and turbulent mixed convection regimes ($0.15 \leq Gr/Re^2 \leq 25$). However, the escalation rate of evaporation decreases with Gr/Re^2 in the forced convection regime whereas in the turbulent mixed convection it increases. In addition, over the range of the free convection regime ($Gr/Re^2 \geq 25$), the evaporation rate is affected not only by the vapour pressure difference but also by the density variation. A dimensionless correlation using the experimental data of all convection regimes ($0.01 \leq Gr/Re^2 \leq 100$) is proposed to cover different water surface geometries and airflow conditions.

Keywords: evaporation rate, forced convection, mixed convection, free convection

1 INTRODUCTION

The evaporation of water into the air is a phenomenon that involves heat and mass transfer. It is of great importance in a wide range of applications such as water purification plants, nuclear engineering, swimming pools, cooling ponds, solar stills, drying systems, and air conditioning. The water evaporation process may be divided into different categories based on the flow regime. The convection mechanisms (natural or forced convection) and the flow regimes (laminar or turbulent flow) impact the rate of evaporation [1, 2]. In general, both natural and forced convection have major effects on the

evaporation process [3, 4]. In order to determine which convection mechanism is the dominant one, the following expression can be used

$$\frac{Gr}{Re^2} = \frac{\text{Natural convection strength}}{\text{Forced convection strength}} \quad (1)$$

where Gr and Re are the Grashof and Reynolds numbers, respectively, which can be determined as follows

$$Gr = \frac{\bar{\rho}_g(\rho_{g,s} - \rho_{g,\infty})gh_D^3}{\mu^2} \quad (2)$$

$$Re = \frac{\bar{\rho}_g V h_D^3}{\mu} \quad (3)$$

where $\rho_{g,s}$ and $\rho_{g,\infty}$ are the densities of moist air at the surface of the water and at ambient conditions, respectively. V , μ , and h_D are the wind velocity, the

*Corresponding author: Faculty of Engineering, Ferdowsi University of Mashhad, P.O. Box No. 91775-1111, Mashhad, Iran.
email: Amin.jodat@yahoo.com

viscosity, and the hydraulic diameter of the test chamber. The density of the moist air at the free surface is the sum of the partial densities of vapour ($\rho_{v,s}$) and dry air ($\rho_{a,s}$) that is [5]

$$\rho_{g,s} = \rho_{v,s} + \rho_{a,s} \quad (4)$$

The mean mixture of air in the boundary layer ($\bar{\rho}_g$) can be determined as [5]

$$\bar{\rho}_g = \frac{\rho_{g,s} + \rho_{g,\infty}}{2} \quad (5)$$

The hydraulic diameter (h_D) is defined as a function of the height (H) and the width (W) of the test chamber

$$h_D = \frac{4WH}{2(W+H)} \quad (6)$$

If Gr/Re^2 is approximately one, the convection regime is a combination of both natural and forced convection regimes [6]. For the forced convection regime, Gr/Re^2 is much less than one while for the natural convection, Gr/Re^2 is much greater than one [6].

Considerable efforts have been made to correlate water evaporation rate from a free water surface with different convection regimes [1, 7–18]. Table 1 is a summary of the proposed correlations and the experimental conditions discussed in the literature. As can be deduced from the table, most of the previous water surface evaporation measurements in wind tunnels have used small evaporation pans [13, 14, 16]. Moreover, the air velocities considered in those investigations are so high (e.g. 1–10 m/s) that they diminish the influence of free convection [1]. This means that in those experiments the forced convection regime heavily dominates the free convection regime. On the other hand, other researchers such

as [7, 15, 17] have performed their experiments in low air velocities, which do not cover the forced convection regime. The complex treatment required for mixed convection [19] has meant that relatively few studies have been published in this convection regime [1, 5]. It can be concluded that the Gr/Re^2 range used in the literature does not cover all convection regimes [8].

The most commonly used correlations to predict water evaporation rate, are those that are based on Dalton's approach [20]. Dalton stated that the evaporation rate of water is proportional to the difference between the vapour pressure at the surface of the water and that at the ambient air and he also noted that the velocity of the wind affects this proportionality. The general form of Dalton's semi-empirical correlation is as follows [20]

$$\dot{m}_e = \frac{(C_1 + C_2)(P_{v,s} - \varphi P_{v,\infty})}{h_{fg}} \quad (7)$$

where \dot{m}_e is the water evaporation rate, $P_{v,s}$ and $P_{v,\infty}$ are the saturated vapour pressure at the free surface and at ambient conditions, respectively, φ is the relative humidity, and h_{fg} is the latent heat of evaporation. C_1 and C_2 are constants which are determined experimentally [18].

Numerous researchers have expressed their results based on Dalton's description [7, 8, 15, 21]; however, there are discrepancies between the coefficients presented by these researchers. One possible reason for these discrepancies is that they are a result of the multiple parameters embedded in the values of the coefficients, such as the area of the body of water and its shape. Another possible reason is that the evaporation rate is not a simple linear function of the vapour pressure difference [18]. A non-linear dependency of evaporation rate (\dot{m}_e) on the vapour

Table 1 Summary of the proposed correlations and the experimental conditions reported in the literature

Reference	Experimental conditions				Proposed correlation
	Evaporating pan size	Air velocity (m/s)	Air temp. range (°C)	Water temp. range (°C)	
Rohwer [7]	0.84 m ² pan	0–0.67	7.1–16.5	6.1–17.2	$\dot{m}_e = (0.125 + 0.755V) \left(\frac{P_{v,s} - \varphi P_{v,\infty}}{1000} \right)$
Hinchley and Himus [13]	0.023–0.07 m ²	0.95–5.8	—	20–70	$\dot{m}_e = (0.2325 + 0.101V) \left(\frac{P_{v,s} - \varphi P_{v,\infty}}{1000} \right)$
Boelter <i>et al.</i> [14]	0.3 m diameter	0	18.7–24.7	20–90	$\dot{m}_e = 0.074 \left(\frac{P_{v,s} - \varphi P_{v,\infty}}{1000} \right)^{1.22}$
Pauken <i>et al.</i> [15]	1.2 m diameter 0.25 m depth	0.1–0.15	20	25–50	$\dot{m}_e = 0.035(C_S - Ca)^{1.237}$
Al-Shamimiri [16]	0.575 m length 0.195 m width 0.1 m depth	2, 3, 4	The room temp.	25–60	$\dot{m}_e = \left(0.120836V^{1.478} \right) \left(\frac{P_{v,s} - \varphi P_{v,\infty}}{1000} \right)^{0.654}$
Shah [17]	It was derived using the analogy theory	0	6–35	7–94	$\dot{m}_e = C \rho_w (\rho_r - \rho_w)^{\frac{1}{3}} (W_r - W_w)$
Tangand Etzion [18]	0.116 m length 0.116 m width 0.22 m depth	0.5–1–1.5	18–40	18–40	$\dot{m}_e = 3600(0.2253 + 0.24644V)(P_{v,s} - \varphi P_{v,\infty})^{0.82}$
Carrier [27]	—	0–7.1	—	—	$\dot{m}_e = \frac{3370(95 + 83.7V)(P_{v,s} - \varphi P_{v,\infty})}{h_{fg}}$

pressure difference has been considered by several researchers [18, 21–23] and as a result considerable modifications have been made to Dalton's theory so that it now has the form of

$$\dot{m}_e = \frac{(C_1 + C_2 V)(P_{v,s} - \varphi P_{v,\infty})^n}{h_{fg}} \quad (8)$$

The majority of researchers have considered the exponent n to have a constant value [8, 14, 16, 18]. However, the exact value of n is in dispute with some analyses indicating that it is less than one [16, 18, 23] while others propose a value greater than one [15, 17]. These discrepancies can originate from the fact that measurements were performed for a limited range of Gr/Re^2 , as pointed out in the comments in Table 1.

The present study on evaporation measurements was motivated by the need to assess the applicability of the widely used evaporation correlations over a wide range of convection regimes ($0.01 \leq Gr/Re^2 \leq 100$). Mathematical modifications to Dalton-based correlations to evaluate the free water surface evaporation rate are proposed for the forced, mixed, and natural convection regimes. In addition, a dimensionless correlation using experimental data on all convection regimes ($0.01 \leq Gr/Re^2 \leq 100$) is proposed to cover different water surface geometries and airflow conditions.

2 MATHEMATICAL CALCULATIONS

The thermal and concentration boundary layers are the main features that appear in the airflow over the free surface of water. The dimensionless governing equations are as follows [24]

$$\rho^* \frac{dT^*}{dt} = \frac{1}{Re \times Pr} \nabla(k^*, \nabla^* T^*) \quad (9)$$

$$\rho^* \frac{dC^*}{dt} = \frac{1}{Re \times Sc} \nabla(D^*, \nabla^* C^*) \quad (10)$$

where ρ^* , k^* , D^* , T^* and C^* are the dimensionless density, conductivity, mass diffusivity, temperature and concentration fields, respectively, and Pr and Sc are the Prandtl and Schmidt numbers which are defined as [24]

$$Pr = \frac{\nu}{\alpha}, \quad Sc = \frac{\nu}{D_{H_2O,air}} \quad (11)$$

where ν , α and $D_{H_2O,air}$ are the kinematic viscosity, and thermal and mass diffusivities, respectively. The dimensionless numbers mentioned in equations (9) and (10) play a significant role in the evaporation of water. In addition, the Nusselt and Sherwood numbers are dimensionless groups that are widely used.

They are defined as a function of Reynolds, Prandtl, and Schmidt numbers as [6]

$$Nu = \frac{h_D}{k} = f(Re, Pr) \quad (12)$$

$$Sh = \frac{g_{m,H_2O} h_D}{\rho D_{H_2O,air}} = g(Re, Sc) \quad (13)$$

where h and g_{m,H_2O} are the heat convection coefficient and the mass transfer coefficient. In addition, the binary diffusion coefficient can be calculated as follows [6]

$$D_{H_2O,air} = 1.87 \times 10^{-10} \left(\frac{T^{2.072}}{P} \right) \quad (14)$$

In order to calculate the mass transfer coefficient, an analogy between heat and mass transfer results in the following expression [6]

$$g_{m,H_2O} = \frac{\dot{m}_e}{m_{f,H_2O,\infty} - m_{f,H_2O,s}} \quad (15)$$

where $m_{f,H_2O,\infty}$ and $m_{f,H_2O,s}$ are the mass fractions of water within the air and in the saturated form, respectively

$$m_{f,H_2O,\infty} = \frac{18.02 X_{H_2O,\infty}}{[18.02 X_{H_2O,\infty} + 28.96(1 - X_{H_2O,\infty})]} \quad (16)$$

$$m_{f,H_2O,s} = \frac{18.02 X_{H_2O,s}}{[18.02 X_{H_2O,s} + 28.96(1 - X_{H_2O,s})]} \quad (17)$$

where X_{H_2O} is the vapour mole fraction which is a function of the vapour pressure (P_{H_2O}) and the atmosphere pressure (P_{atm})

$$X_{H_2O} = \frac{P_{H_2O}}{P_{atm}} \quad (18)$$

In order to evaluate the saturated vapour pressure ($P_{v,s}$) as a function of temperature, the following relation may be used [25]

$$P_{v,s} = 10^5 \exp \left[65.832 - 8.2 \ln(T_s) + 5.717 \times 10^{-3} T_s - \frac{7235.46}{T_s} \right] \quad (19)$$

where T_s is the free surface temperature.

A barometer was used to measure the total pressure in the laboratory for each experiment. In addition, in order to calculate the density of moist air, the perfect gas equation was employed.

In the present study, the Sherwood number for the mixed convection flow regime ($Gr/Re^2 \cong 1$) was defined as [6]

$$\frac{Sh_{\text{mixed}}}{Sh_{\text{free}}} = \left[1 + \left(\frac{Sh_{\text{forced}}}{Sh_{\text{free}}} \right)^a \right]^{1/a} \quad (20)$$

where a is an exponent which can vary in the range between one and two [1]. Sh_{free} and Sh_{forced} are the Sherwood numbers for the free and forced convection flow regimes and they can be defined as

$$Sh_{\text{free}} = 0.14(Gr Sc)^{0.33} \quad (21)$$

$$Sh_{\text{forced}} = 0.034Sc^{0.33}Re^{0.8} \quad (22)$$

It should be noted that the flow regime was turbulent in the free convection regime since the mass-based Grashoff number (equation (2)) ranged from 2.1×10^8 to 6.7×10^9 . Also, due to the existence of a series of baffles which were placed in the upstream end of the wind tunnel, the air flow regime in the forced convection regime was turbulent. Therefore, equations (21) and (22) are valid for the turbulent flow regime.

3 EXPERIMENTAL MEASUREMENTS

The experimental measurements were carried out in a test chamber with internal dimensions of $150 \times 100 \times 100$ cm. The pond depth in the test chamber was 25 cm. A schematic of the test chamber is shown in Fig. 1. The large size of the evaporation pan used in this investigation reduced convective edge effects. Small pans have a greater portion of their interior surface affected by convection due to density gradients around the pan edges [8]. In order to reduce the heat loss via conduction, the pond was made up of medium-density fibre-board and the

whole test chamber was isolated using the polystyrene panels of 5 cm in thickness. An aluminium foil tape was used within the interior surfaces to reduce the radiative heat loss and prevent water vapour absorption.

Two immersion heaters were installed near the bottom of the pan to elevate the water temperature to the desired conditions. They were low heat flux heaters with 2500 W of total power each. The heaters were made of nichrome wire encased in poly(tetrafluoroethylene) spaghetti tubing.

A draw-thru centrifugal fan was used to exhaust the air and control the wind velocity within the chamber. Draw-thru fans have the advantage of reducing the extent to which turbulence affects the evaporation rate. The evaporation rate was evaluated based on two methods. First, the flowrate and the difference between the inlet and outlet absolute humidity were used. Second, with the help of a small pan which was connected to the main pond via a siphon tube [15]. The evaporation rate was calculated based on weighing this small pan using a digital scale over a 10 min period of time. The maximum capacity and the resolution of the scale were about 4 kg and 0.01, respectively. However, when the evaporation rate was too slow the measurements were recorded on an hourly basis.

The mean surface water temperature was measured by averaging the readings of eight T-type thermocouples that were placed 4 cm below the water surface. The pan was divided into eight equal square sections and one thermocouple was placed in the centre of each section. The water temperatures

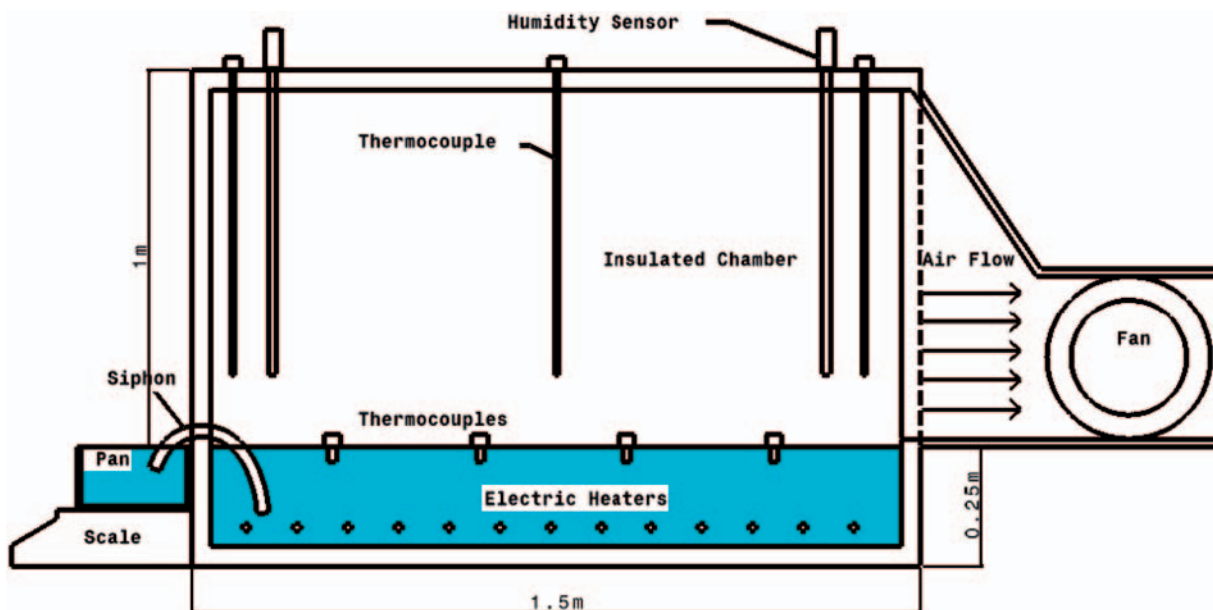


Fig. 1 Experimental test chamber

considered in this investigation ranged from 20 to 55°C in approximately 2.5°C increments. A thermoregulation system was used to guarantee a temperature oscillation of the water of about $\pm 0.1^\circ\text{C}$ from the fixed value.

Air relative humidity was measured by two sensors placed at the inlet and outlet of the wind tunnel, 25 cm above the water surface. In addition, the air temperature was measured by a thermocouple located over the mid-point of the evaporation pan.

The air velocity within the chamber was measured using a thermal anemometer, at nine locations across the water surface at about 15 mm above the water surface, and the maximum deviation observed was less than 10 per cent. The average air velocities considered were 0.05, 0.1, 0.3, 0.9, 1.5, 2, 4, 5, and 6 m/s. The inlet air temperature and relative humidity were controlled using a conventional air conditioning system. The specifications of the devices are presented in Table 2. All the measuring instruments were calibrated before the experiments were performed and the data generated by these instruments was captured using a PC data acquisition system.

4 RESULTS AND DISCUSSIONS

A wide range of flow regimes namely free, mixed, and forced convection ($0.01 \leq Gr/Re^2 \leq 100$) were studied to reveal the validity of the Dalton approach-based correlations. This relatively wide range of Gr/Re^2 was produced using air average velocities of 0.05, 0.1, 0.3, 0.9, 1.5, 2, 4, 5, and 6 m/s and the water temperatures from 20 to 55°C. Figure 2 displays the variation of the evaporation rate based on the vapour pressure difference for the free convection regime ($Gr/Re^2 \geq 25$) in which the wind velocity is 0.05 and 0.1 m/s. As seen in the figure, the data do not follow a specific trend. The scattering of the results shows that the evaporation rate is not a simple function of vapour pressure difference in the free convection regime. In fact, in that regime both the vapour pressure difference and the density difference between the water's surface and the ambient air affect the evaporation

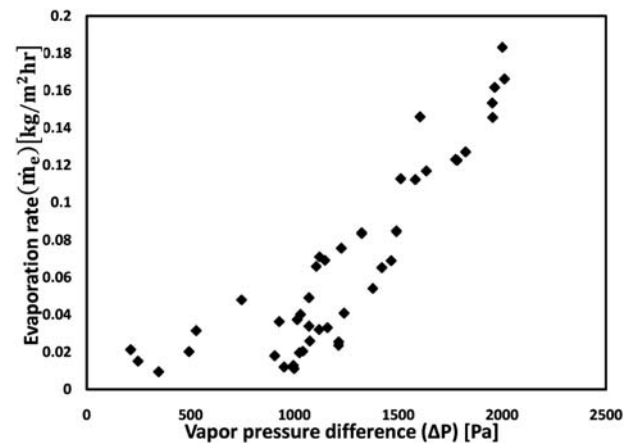


Fig. 2 Evaporation rate against the vapour pressure difference for the free convection regime ($V \leq 0.1$ m/s and $Gr/Re^2 \geq 25$)

rate. This dependency of the evaporation rate on the density difference has been previously reported in the literature [17], therefore, Dalton approach-based models (equation (7)) which do not take into account the effect of vapour density difference, are not able to satisfactorily predict the results obtained in this convection regime. To take into account the effects of both vapour pressure difference and density difference, $\dot{m}_e/\Delta P^{1.05}$ for experimental data is plotted as a function of the density difference in Fig. 3. From this figure it can be seen that $\dot{m}_e/\Delta P^{1.05}$ increases as a power function with increasing density difference. Considering the density difference effect on the evaporation rate, a new modified correlation for the free convection regime ($Gr/Re^2 \geq 25$ and $V \leq 0.1$ m/s) is suggested as follows

$$\dot{m}_e = 0.01 C (P_{v,s} - \varphi P_{v,\infty})^n (\rho_{g,s} - \rho_{g,\infty})^{n'} \quad (23)$$

Performing a non-linear regression [26] on the experimental data it was found that the best fit value of the unknown constants to all measurements were

$$C = 0.069, \quad n = 1.105, \quad n' = 0.153$$

Table 2 Specifications of the experimental apparatus

The experimental apparatus	Manufacturer	Type	Range	Accuracy
Digital balance	Bel Engineering	Ultra Mark 4000	0 to 4 kg	± 0.01 g
Humidity sensors	Ohmic instruments	HS Series	1 to 99%	± 1 % RH
Temperature sensors	Testo	T-type thermocouples	-50 to $+199.9^\circ\text{C}$	0.1°C
Thermal anemometer	Testo	Testo 400	0 to $+20$ m/s	± 0.01 m/s (0 to $+1.99$ m/s) ± 0.02 m/s ($+2$ to $+4.9$ m/s) ± 0.04 m/s ($+5$ to $+20$ m/s)
Air conditioning system	Atlas Pars Air Conditioning Co.	AAHC-04	—	—
Centrifugal fan	Pars Fan Hoonam	PCB SWS	Maximum capacity - 15000 cfm	—

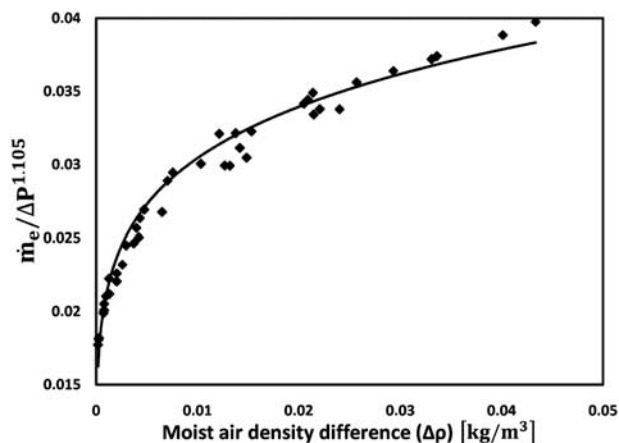


Fig. 3 The effect of moist air density difference on the proposed modified evaporation rate ($\dot{m}_e / \Delta P^{1.105}$) for the free convection regime $V \leq 0.1$ m/s and $Gr/Re^2 \geq 25$

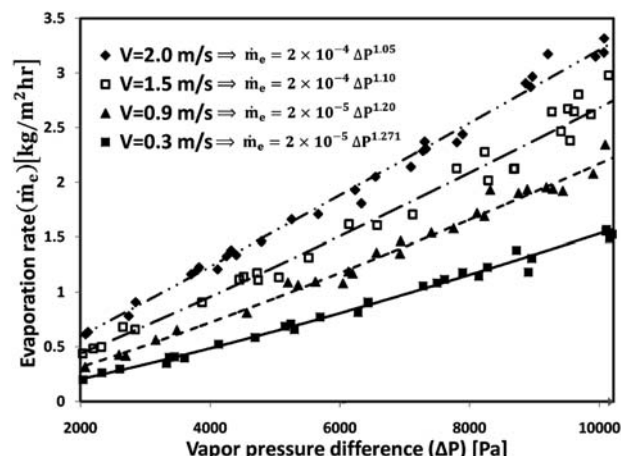


Fig. 5 Evaporation rate against the vapour pressure difference for various wind velocities of the mixed convection regime ($0.15 \leq Gr/Re^2 \leq 25$)

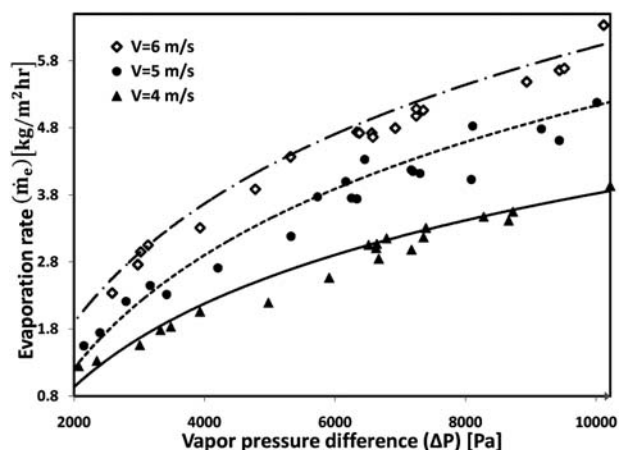


Fig. 4 Evaporation rate versus the vapour pressure difference for various wind velocity of the forced convection regime ($0.01 \leq Gr/Re^2 \leq 0.1$)

Figure 4 demonstrates the influence of the vapour pressure difference and wind velocity on the evaporation rate for the forced convection regime ($0.01 \leq Gr/Re^2 \leq 0.1$). As shown in the figure, the evaporation rate increases as a power function with increase in the vapour pressure difference. The exponent n in equation (8) is less than one for this flow regime, since the slope of the curves reduces with the vapour pressure difference. In addition, the evaporation rate increases with the wind velocity. These results also show that Dalton approach-based correlations without modification are unable to predict the non-linear variation of evaporation rate with vapour

pressure difference. This is in agreement with the experimental data of Al-Shamimiri. [16], Tang and Etzion [18], and Marek and Straub [23]. These researchers have suggested that the value of n in equation (8) must be less than one.

The effect of the vapour pressure difference on the evaporation rate for the mixed convection regime ($0.15 \leq Gr/Re^2 \leq 25$) is shown in Fig. 5. As shown in the figure, the slope of the curves, which are fitted to the experimental data, increases with the vapour pressure difference; therefore the exponent n in the modified Dalton model (equation (8)) is greater than one which is in accordance with Paukan [1], Boetler *et al.* [14], and Moghiman *et al.* [22]. However, the exponent n can be represented more accurately if it is considered to be a function of air velocity. A non-linear regression using SPSS software resulted in the following mathematical model for the water evaporation rate

$$\dot{m}_e = 0.001(0.032\ 62V^3 + 0.018\ 14V^2 + 0.048\ 18V + 0.022\ 64)(\rho_{g,s} - \varphi\rho_{g,\infty})^{(0.009V^2 - 0.132V + 1.186)} \tag{24}$$

It must be noted that this correlation is valid for both mixed and forced convection regimes for the cases considered in the present study ($0.15 \leq Gr/Re^2 \leq 25$ and $0.3 \leq V \leq 6$).

A comparison of the proposed model (equation (24)) and those in the literature [7, 13, 16] for both forced and mixed convection regimes is presented in Figs 6 and 7, respectively. As shown in these figures, the predicted evaporation rates

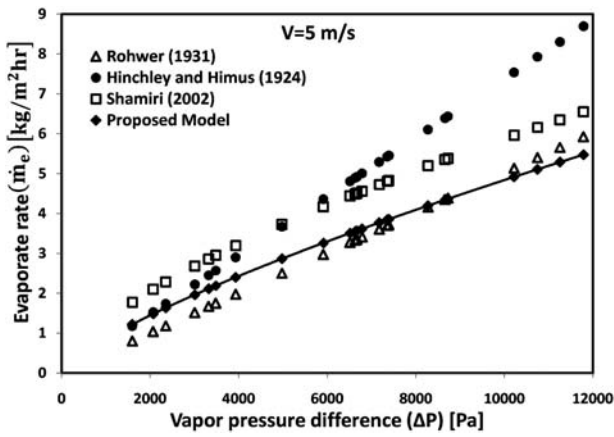


Fig. 6 Comparison of the evaporation rate between the proposed model and those in the literature [7, 13, 16] for the forced convection regime and wind velocity $V=5\text{ m/s}$

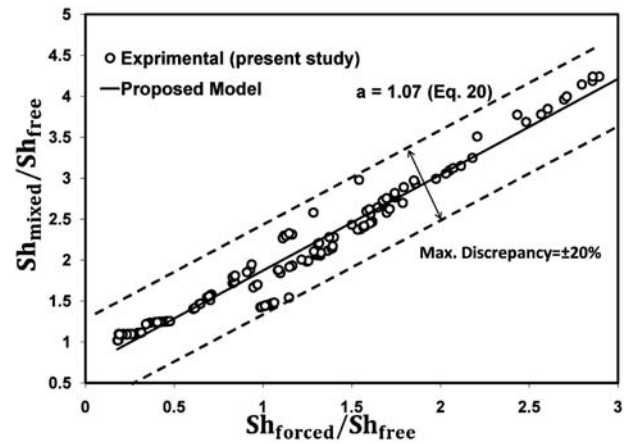


Fig. 8 The effect of $Sh_{\text{forced}}/Sh_{\text{free}}$ on $Sh_{\text{mixed}}/Sh_{\text{free}}$ based on the experimental results for the mixed convection regime (equation (20))

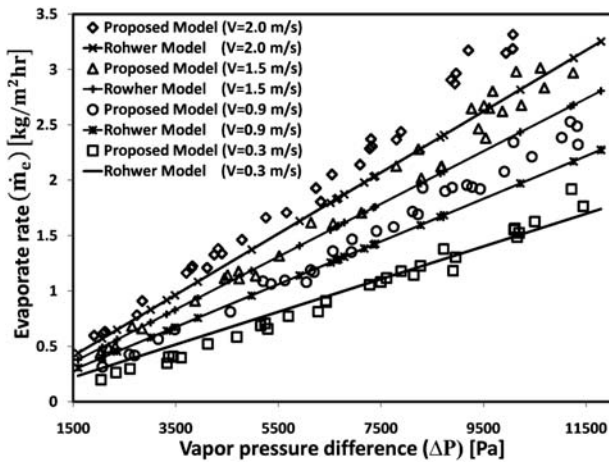


Fig. 7 Comparison of the evaporation rate between the proposed model and those in the literature [7] for the mixed convection regime and various wind velocities

results from Hinchley and Himus [13]. and Al-Shammiri [16] are higher than the experimental data of the present study, while the predictions of Rohwer [7] are closer to the measured data. This can be explained as follows. The experiments of Hinchley and Himus [13] were conducted with relatively small pans with surface areas on the order of $0.02\text{--}0.07\text{ m}^2$. The edge effects caused by the small pan sizes may be one of the reasons for the large evaporation rates predicted by their correlation [8]. In the experiments of Al-Shammiri [16], the highly turbulent conditions caused by the fan that operated in the blow-thru mode can be a reason for his correlation to over-predict the evaporation rate. The small discrepancy between the experimental data and the Rohwer model [7] is probably due to the fact that the

non-linear dependency of evaporation rate on the vapour pressure difference was not considered in his model (exponent $n=1$). In this study, this non-linearity has been taken into account in equation (24), and it is a good approximation for high air velocities and a rough estimate for lower air velocities.

Figure 8 shows the ratio of $Sh_{\text{total}}/Sh_{\text{free}}$ versus the ratio of $Sh_{\text{forced}}/Sh_{\text{free}}$ calculated based on the experimental evaporation data for the mixed convection regime ($0.15 \leq Gr/Re^2 \leq 25$) i.e. in the plot $Sh_{\text{total}} = Sh_{\text{mixed}}$. The free and forced convection components of the Sherwood number are calculated from equations (21) and (22), respectively. Attention should now be paid to find the optimal value of exponent a in equation (20). Repeating the non-linear regression for different values of a , it is concluded that the best fit value of a (in equation (20)) to all measured data for the mixed convection regime is $a=1.075$. The maximum discrepancy between the experimental data and the best exponent found for equation (20) is ± 20 per cent.

In Fig. 9, the ratio of total Sherwood number to the Sherwood number for the free convection regime $Sh_{\text{total}}/Sh_{\text{free}}$ versus Gr/Re^2 has been shown. In this figure, the total Sherwood number and the free convection Sherwood number for all data collected in the experiments were calculated using equation (13) and equation (21), respectively. Then the variations of the ratio of $Sh_{\text{total}}/Sh_{\text{free}}$ is plotted versus Gr/Re^2 and the best fit to this curve found to have the following form

$$\frac{Sh_{\text{total}}}{Sh_{\text{free}}} = 1.441 - 0.345 \ln\left(\frac{Gr^2}{Re}\right) + 0.22 \left[\ln\left(\frac{Gr^2}{Re}\right) \right]^2 - 0.037 \left[\ln\left(\frac{Gr^2}{Re}\right) \right]^3 \quad (25)$$

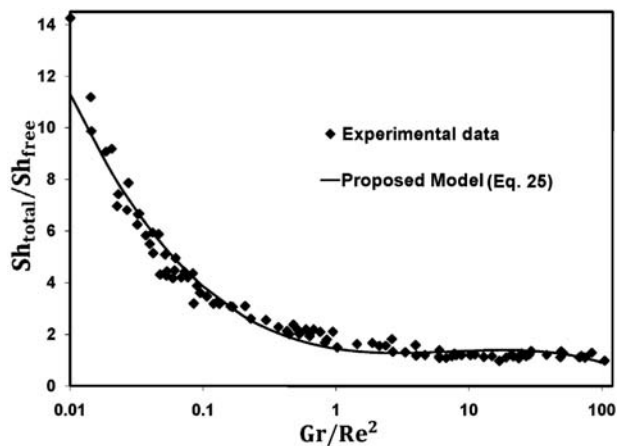


Fig. 9 Comparison of the proposed model (equation (25)) and the experimental data for the $0.01 \leq Gr/Re^2 \leq 100$

Table 3 The applicability range for equations (23) to (25) Equation

	Applicability range
Equation (23)	$0.3 \leq V \leq 5 \text{ m/s}$ $20 \leq$ water temperature $\leq 55^\circ\text{C}$ $0.01 \leq Gr/Re^2 \leq 25$
Equation (24)	$V \leq 0.1 \text{ m/s}$ $20 \leq$ water temperature $\leq 55^\circ\text{C}$ $Gr/Re^2 > 25$
Equation (25)	$0.05 \leq V \leq 5 \text{ m/s}$ $20 \leq$ water temperature $\leq 55^\circ\text{C}$ $0.01 \leq Gr/Re^2 \leq 100$

Equation (25) is valid for a wide range of convection regimes ($0.01 \leq Gr/Re^2 \leq 100$). This dimensionless correlation allows the results of this study to be extended to other evaporation conditions (variation in surface geometry and airflow conditions) rather than those described here.

The applicability range for equations (23) to (25) are presented in Table 3.

5 CONCLUSIONS

In the present paper, the validity of the application of Dalton approach-based models to calculate the rate of water evaporation is assessed by performing experimental measurements in different evaporation regimes. A wide range of Gr/Re^2 ($0.01 \leq Gr/Re^2 \leq 100$) is achieved by applying different air velocities and water temperatures on a heated water pool in a wind tunnel. The following conclusions may be drawn from the presented results.

1. For forced and mixed convection regimes, Dalton approach-based correlations without modification are unable to predict the non-linearity between water evaporation rate and vapour pressure difference.

2. The evaporation rate is a function of the vapour pressure difference with a power law relation in which the exponent n is less than one for the forced convection ($0.01 \leq Gr/Re^2 \leq 0.1$) and is greater than one for the mixed convection regime ($0.15 \leq Gr/Re^2 \leq 25$).
3. Non-linear data analysis indicates that considering the exponent n in equation (8) as a function of wind velocity (as indicated in equation (24)) increases the accuracy of the correlation in the mixed and forced convection regimes.
4. For the free convection flow regime, the evaporation rate is a function of not only the vapour pressure difference but also the density difference of the moist air.
5. There exist other parameters such as size and the shape of the ripples on the free surface which require further investigation.

© Authors 2011

REFERENCES

- 1 **Paukan, M. T.** An experimental investigation of combined turbulent free and forced evaporation. *Exp. Therm. Fluid Sci.*, 1999, **18**, 334–340.
- 2 **Debbissi, C., Orfi, J., and Nasrallah, S. B.** Evaporation of water by free or mixed convection into humid air and superheated steam. *Int. J. Heat Mass Transf.*, 2003, **46**, 4703–4715. (DOI: 10.1016/S0017-9310(03)00092-9).
- 3 **Liu, J., Aizawa, Y. and Yoshin, H.** Experimental and numerical study on indoor temperature and humidity with free water surface. *Energy Build.*, 2005, **37**, 383–388.
- 4 **Steeman, H. J., Joen, C., Van Belleghem, M., Janssens, A. and De Paepe, M.** Evaluation of the different definitions of the convective mass transfer coefficient for water evaporation into air. *Int. J. Heat Mass Transf.*, 2009, **52**, 3757–3766. (DOI: 10.1016/j.ijheatmasstransfer.2009.01.047).
- 5 **Iskra, C. R. and Simonson, C. J.** Convective mass transfer coefficient for a hydro dynamically developed airflow in a short rectangular duct. *Int. J. Heat Mass Transf.*, 2007, **50**(11–12), 2376–2393. (DOI: 10.1016/j.ijheatmasstransfer.2006.10.026).
- 6 **Lienhard, J. H. and Lienhard, V. J. H.** *A heat transfer textbook*, 3rd edn, 2005 (Phlogiston Press, New York).
- 7 **Rowher, C.** Evaporation from free water surface, US Department of Agriculture in cooperation with Colorado Agricultural Experiment Station. *Tech. Bull.*, 1931, **271**, 96–101.
- 8 **Sartori, E. A.** Critical review on equations employed for the calculation of the evaporation rate from free water surfaces. *Solar Energy*, 2000, **68**, 77–89.
- 9 **Asdrubali, F. A.** Scale model to evaluate water evaporation from indoor swimming pools. *Energy Build.*, 2008, **41**, 311–319. (DOI: 10.1016/j.enbuild.2008.10.001).

- 10 **Chuck, W.** and **Sparrow, E. M.** Evaporative mass transfer in turbulent forced convection duct flows. *Int. J. Heat Mass Transf.*, 1987, **30**(2), 215–222.
- 11 **Tanny, J., Cohen, S., Assouline, S., Lange, F., Grava, A., Berger, D., Teltch, B.** and **Parlange, M. B.** Evaporation from a small water reservoir: direct measurements and estimates. *J. Hydrol.*, 2008, **351**, 218–229. (DOI: 10.1016/j.jhydrol.2007.12.012).
- 12 **Miller, W. A.** and **Atchley, J. A.** A correlation for laminar, low-temperature, gradient heat transfer applied to a low slope roof, in normal performance of the exterior envelope of buildings. In Proceedings of ASHRAE THERM VIII, Clearwater, Florida, 2001, vol. 3, pp. 26–34.
- 13 **Hinchley, J. W.** and **Himus, G. W.** Evaporation in currents of air. *J. Soc. Chem. Ind.*, 1924, **7**, 57–63.
- 14 **Boetler, L. M. K., Gordon, H. S.** and **Griffin, J. R.** Free evaporation into air of water from a free horizontal quiet surface. *Ind. Engng. Chem.*, 1946, **38**(6), 596–600.
- 15 **Pauken, M. T., Tang, T. D., Jeter, S. M.** and **Abdel-Khalik, S. I.** A novel method for measuring water evaporation into still air. *ASHRAE Trans.*, 1993, **99**(1), 297–300.
- 16 **Al-Shamimiri, M.** Evaporation rate as a function of water salinity. *Desalination*, 2002, **150**, 189–203.
- 17 **Shah, M. M.** Rate of evaporation from undisturbed water pools to quiet air: evaluation of available correlations. *Int. J. HVAC&R*, 2002, **8**, 125–131.
- 18 **Tang, R.** and **Etzion, Y.** Comparative studies on the water evaporation rate from a free water surface and that from a free surface. *Build. Environ.*, 2004, **39**, 77–86.
- 19 **Shah, M. M.** Prediction of evaporation from occupied indoor swimming pools. *Energy Build.*, 2003, **35**, 707–713.
- 20 **Dalton, J.** Experimental essays on the constitution mixed gases; on the force of steam or vapor from water and other liquids in different temperatures, both in a Torricellian vacuum and in air; on evaporation and on the expansion of gases by heat. *Mem. Manchester Liter. Phil. Soc.*, 1802, **535–602**(11), 535–602.
- 21 **Moghiman, M.** and **Jodat, A.** Effect of air velocity on water evaporation rate in indoor swimming pools. *The Iranian Society of Mechanical Engineers*, 2007, **8**, 19–30.
- 22 **Moghiman, M., Jodat, A.,** and **Javadi, M.** Experimental investigation of water evaporation in indoor swimming pools. *Int. J. Heat Mass Technol.*, 2007, **25**(2), 43–47.
- 23 **Marek, R.** and **Straub, J.** Analysis of the evaporation coefficient and the condensation coefficient of water. *Int. J. Heat Mass Transf.*, 2001, **44**, 39–53.
- 24 **Incropera, F. P.** and **Dewitt, D. P.** *Fundamentals of heat and mass transfer*, 2002 (John Wiley and Sons, New York).
- 25 **Boukadida, N.** and **Nasrallah, S. B.** Mass and heat transfer during water evaporation in laminar flow inside a rectangular channel—validity of heat and mass transfer analogy. *International Journal of Thermal Sciences*, 2001, **40**, 67–81.
- 26 **Seber, A. F.** and **Wild, C. J.** *Nonlinear regression*, 2003 (John Wiley & Sons, New York).
- 27 **Carrier, W. H.** The temperature of evaporation. *ASHVE Trans.*, 1918, **24**, 25–50.

APPENDIX

Notation

$D_{\text{H}_2\text{O,air}}$	binary mass diffusion coefficient
h_{D}	hydraulic diameter of rectangular duct (m)
g	gravitational acceleration
$g_{\text{m,H}_2\text{O}}$	mass transfer coefficient
Gr	mass transfer Grashof number
h_{fg}	enthalpy of vaporization (J/kg)
H	height of rectangular duct (m)
K	thermal conductivity
L	length of water pan (m)
\dot{m}_{e}	evaporation rate of water
$m_{f,\text{H}_2\text{O}}$	the mass fractions of water
Nu	Nusselt number
P	pressure (Pa)
Pr	Prandtl number
$P_{\text{v,s}}$	saturated vapor pressure at the water surface
$P_{\text{v},\infty}$	saturated vapor pressure at the ambient air
R^2	Correlation coefficient
Re	Reynolds number
Sc	Schmidt number
Sh	Sherwood number
t	time (h)
T	temperature (K)
T_{s}	free surface temperature (K)
V	velocity of air
W	width of the test chamber
$X_{\text{H}_2\text{O}}$	vapour mole fraction
μ	dynamic viscosity
ρ	density
$\bar{\rho}$	mean mixture density of air
φ	relative humidity
Subscripts	
free	free convection flow regime
forced	forced convection flow regime
g	moist air property including dry air and water vapour
mixed	mixed convection flow regime
s	properties at the surface of the water
total	sum of free and forced convection component
∞	average properties at the ambient air